

Mao S. Wu and S. Shyam Sunder  
Massachusetts Institute of Technology, Department of Civil Engineering,  
Room 1-274, Cambridge, MA 02139

## CONSTITUTIVE MODELING OF POLYCRYSTALLINE ICE

### Abstract

This paper examines the constituent elements of a numerical model for simulating ice-structure interaction processes. The discussion emphasizes the fundamental element of the model, i.e., the constitutive model, and compares the micromechanical approach to the macroscopic approach which is phenomenological but physically motivated. The appeal for the latter approach is underlined by the computational intractability of a micromechanical model in a complex initial- and boundary-valued problem, and the incomplete knowledge of the physical mechanisms of deformation in ice. The physically motivated phenomenological approach is elaborated in this paper using as an example the thermodynamic constitutive model proposed by Shyam Sunder and Wu (1988a, b) for flow in polycrystalline ice. Phenomenological equations have also been used to describe inelastic deformations of metals during hot-working (Brown et al., 1988), and of glassy polymers near the glass transition temperature (Boyce et al., 1988). Also discussed are the physical interpretation of material parameters and their determination from standard tests on ice, and the validation of the predictive capabilities of the numerical model.

### 1. INTRODUCTION

The ultimate objective of numerical modeling as applied to ice-structure interaction is the prediction of ice loads on structures. Within this broad objective at least two roles can be identified for a numerical model. The first is the simulation of field-scale problems without necessarily having to conduct field-scale experiments. This allows one to explore the sensitivity of the ice-structure response to various input parameters associated with the structure, materials and environment at comparatively little cost. Furthermore, a wide range of behaviors can be studied under controlled conditions, particularly those related to extreme conditions of loading.

A second role of numerical modeling is to help establish more rational engineering design procedures that lead to safe and economical systems. For instance, a parametric study enables the identification of field parameters (such as speed of ice feature, ice strength and interaction geometry) that have the most significant effect on the predicted ice force. These parameters could then be obtained with the greatest accuracy, thus improving the accuracy of prediction. Furthermore, on the basis of such studies parametric formulae can be established for design purposes. It may also help to optimize certain

features of the structural system. For instance, if for certain environmental and loading conditions the interaction geometry is found to influence the ice forces significantly, then much effort could be spent on studying the prevalent ice geometry so that the structural geometry could be optimized to minimize ice forces.

The relationships between the various elements of a numerical model are discussed in Section 2. A principal component, the constitutive model, is discussed in Section 3. This attempts to establish the link between phenomenology and the deformation mechanisms operating on the microscale, and points out the current inadequate knowledge concerning physical processes controlling creep in ice. The procedures required for the determination of model parameters and the validation of the numerical model are reviewed in Section 4. The last section summarizes the authors' view on current and future research in constitutive modeling as applied to numerical studies.

## 2. CONSTITUENT ELEMENTS OF A NUMERICAL MODEL

An applied ice mechanics problem generally requires solution by numerical simulations. This is because of the many inherent complexities that must be taken into account in a typical problem. First, ice is a complex material occurring naturally at high homologous temperatures, and generally has several deformation mechanisms operating on the microscale. It may contain cracks, voids, brine channels, and may be texturally anisotropic. Second, the environmental, loading and ice-structure interface conditions must be taken into account as appropriate boundary and initial conditions. These include temperature, velocity of ice feature, and the geometry of contact and the coefficient of friction between ice and structure. Third, the complex geometries of the ice and indenter complicate the prediction of ice forces even further. In some problems, the important parameters are the aspect ratio (between indenter width and thickness of ice feature) and the structural geometry (indenter with vertical or inclined face).

Depending on these parameters and their interdependence, ice displays a wide range of behaviors including transient creep, steady-state creep, tertiary creep, and brittle fracture. During indentation or impact, these complex behaviors can cause ice to fail by creep, crushing, cracking, spalling and buckling. The deformation mode map of Palmer et al. (1983), reproduced in Fig. 1, schematically shows the influence of strain rate and aspect ratio on the deformation mode. It shows that ice fails by creep at strain rates below about  $10^{-4} \text{ s}^{-1}$ . At higher strain rates, it can fail by a variety of modes ranging from crushing for aspect ratios less than about 0.5 to radial and circumferential cracking for aspect ratios greater than about 10.

Approximate analytical methods for indentation problems based on the plastic limit analysis (e.g., Ralston (1978)) and the reference-stress model (e.g., Ponter et al. (1983)) suffer from the drawback that not all the parameters can be simultaneously analyzed. It is in this aspect that numerical models using the boundary and finite element methods offer a definite advantage (Jordaan, 1986). Recent work by Shyam

Sunder et al. (1989), which combines a viscoplastic flow model and a smeared cracking model of tensile failure in a finite element framework, is a step towards the study of ice-structure interaction in the ductile-to-brittle transition region.

The constituent elements or building blocks of a numerical model are the constitutive, finite element (or boundary element), and the system models. At the lowest level is the constitutive model which determines the response of a material subjected to a given excitation. Two distinct types of constitutive models exist: the macroscopic model and the micromechanical model.

In the macroscopic approach, a material sample is regarded as uniform and its deformation and stress fields are compatible with the boundary conditions. Constitutive relations are derived for and applied to the particles of the continuum. A continuum particle refers to a representative volume of the neighborhood of the material point. In a polycrystalline (possibly heterogeneous) sample the representative volume must be sufficiently large to permit the overall behavior of the sample to be adequately described, and yet appropriately small to allow the various microscopic heterogeneities to be distinguished. For instance, the grains in polycrystalline ice are highly heterogeneous with different crystallographic orientations, thus requiring a sufficiently large representative volume for the continuum theories to apply. However, internal stresses caused by local heterogeneities such as the pile-up of dislocations moving on basal planes are of importance since they may initiate flow on nonbasal planes or microcracking. Too large a representative volume may average out the contributions of these local stresses.

A macroscopic model can be purely phenomenological, or phenomenological but physically motivated. An example of the former is one of the many classical spring-dashpot models. In a physically motivated approach, the constitutive relations are derived from the viewpoint of the underlying mechanisms of deformation (which may be represented phenomenologically by springs and dashpots). The flow models of Sinha (1978), Michel (1978), and Ashby and Duval (1985) for polycrystalline ice are in this category. This approach has also been adopted by Brown et al. (1988) for modeling the inelastic behavior of metals during hot-working, and by Boyce et al. (1988) in their constitutive model for glassy polymers near the glass transition temperature.

In the micromechanical approach, constitutive relations are derived for suitable "microelements", and averaging procedures are used to derive the overall macroscopic response. In addition, the characterization of the overall response requires the description of the local quantities for a typical microelement in terms of the far-field boundary data. Taking plasticity in metals as an example, and if the overall inelasticity is due to slip over crystallographic planes in individual crystals, one approach is to derive the constitutive relations for the microelements using local continuum parameters which are functions of quantities characterizing local processes such as the rates of slip in the various slip systems. The work of Rice (1971) provides a foundation for constitutive modeling of inelastic deformations as a

consequence of structural rearrangements occurring on the microscale. For crystalline slip in metals structural rearrangements are due to the incremental glide motions of the dislocations. Using discrete structural variables which represent specific structural rearrangements and assuming that the rate of each rearrangement depends on stress through its own conjugate force, or more specifically, the rate of slip on a given slip system is dependent on the resolved shear stress on that system, it was shown that a normality structure exists in the macroscopic constitutive laws. However, further research is needed for polycrystalline ice since knowledge of the physical processes of deformation is incomplete. This is true for both creep and damage processes. These issues are elaborated in Section 3.

To study ice-structure interaction by means of a numerical model, it is necessary to incorporate the constitutive model in a finite element (or boundary element) framework. This enforces equilibrium of nodal forces and moments as well as compatibility of displacements at the nodes. The choice of a particular finite element type (e.g., plane linear or quadratic isoparametric element, or isoparametric plate element) depends on the application and the requirements of accuracy, efficiency, stability and good convergence characteristics. Viscoplastic constitutive models based on internal state variables are generally stiff, and require efficient time-integration schemes for solution. This efficiency generally demands a minimal acceptable level of accuracy, since a typical problem may involve hundreds of elements and solving the complex models for both creep and cracking for all the elements is costly. Furthermore, this imposes a constraint on the level of complexity of the finite element model.

Finally, at the uppermost level is the system model which encompasses the entire ice feature and the structure. This involves the task of problem definition, i.e., the translation of a complex engineering problem into a system model. Because of the many parameters that have to be dealt with and their statistical nature, a judicious choice must be made which necessarily introduces idealizations. Once the system model is defined, it is integrated with the finite element and constitutive models into a numerical model. This involves optimizing the mesh design using the adopted finite elements. Special elements may be used to simulate the ice-structure interface and crack tip regions. Material constitutive laws and appropriate boundary conditions are specified for the elements.

It may be argued that the levels of complexity for all three models should be comparable. Thus, use of a sophisticated micromechanical model in a numerical framework may not yield solutions of the desirable accuracy since the boundary conditions determined from field data may be susceptible to considerable uncertainties. Moreover, knowledge of the physical processes and their interactions in polycrystalline ice is not yet satisfactory. It is also costly and quite impossible to pursue the details of microstructural changes at all sites within the material and within the time of interest. This, however, is not to say that micromechanical modeling is of secondary importance: if the physics is correctly described a micromechanical model enables accurate and reliable prediction of various phenomena with a consistent set of equations. A purely phenomenological model may describe uniaxial creep response well, but may fail completely with a different kind of loading. These arguments suggest that a physically motivated phenomenological model provides the best compromise. In Section 3 the model proposed by

Shyam Sunder and Wu (1988a, b) is discussed in terms of current knowledge of the physical mechanisms of deformation in polycrystalline ice.

### 3. PHENOMENOLOGICAL AND PHYSICAL MODELS OF CONSTITUTIVE BEHAVIOR

Formulating a micromechanical or physical model requires modeling of the physical processes of deformation at the dislocation or molecular level. For this reason, the molecular structure of ice is first discussed, following Glen (1968). The various physical processes and their models are then discussed in connection with observed macroscopic behavior. Also, the physical bases of various constitutive models (Sinha, 1978; Michel, 1978; Ashby and Duval, 1985; Shyam Sunder and Wu, 1988a, b) are reviewed.

Refer to Fig. 2, reproduced from Glen (1968), for the following discussion. The form of ice at low pressures, i.e., ice I-h, has a hexagonal structure. Each oxygen atom occupies a point of the hexagonal lattice and has four nearest neighbors located at about 0.276 nm away at the corners of a approximately regular tetrahedron. The oxygen atoms are concentrated on the basal planes to which the principal hexagonal axis (c-axis) is perpendicular. Furthermore, each oxygen atom is covalently bonded to two protons at a distance of about 0.1 nm away, forming the water molecule. The same oxygen atom is linked to two other protons about 0.176 nm away by hydrogen bonding.

The structure of ice I-h is such that the oxygen atoms are crystallographically ordered with the positions of the hydrogen atoms obeying the Bernal-Fowler rules which state that (i) only two hydrogen atoms are associated with each oxygen atom and that they can occupy any of the four tetrahedral links between the oxygen atoms, and (ii) only one hydrogen atom can lie between any pair of oxygen atoms. A breach of the first rule produces ionic defects: a negative ion  $(OH)^-$ , or a positive ion  $(H_3O)^+$ . A breach of the second rule produces Bjerrum defects: a D-defect, i.e., a bond with two protons on it, or an L-defect, i.e., a bond with no protons on it.

The sizes, shapes and orientations of crystals in a polycrystal can vary, giving rise to different types of ice. Two of the most common freshwater ice types are the S-2 columnar-grained ice with preferred horizontal orientation of c-axes, and the T-1 snow ice with equiaxed grains and a random orientation of c-axes. The discussion in the following sections is restricted to freshwater polycrystalline ice.

#### 3.1 Elasticity

The classical Hooke's law generalized for three dimensions is generally adopted for the description of pure elastic deformations in ice. This assumes that elastic deformations due to lattice stretching are linearly related to stress by the elastic constants (moduli or compliances). Since ice crystals are transversely anisotropic with respect to their elastic properties, five independent elastic constants are required to describe elasticity in single crystals. For isotropic polycrystalline ice only two elastic constants

are required. Those in use include Young's modulus and Poisson's ratio, or the bulk modulus and the shear modulus.

The elastic constants of polycrystalline ice are dependent on physical parameters such as temperature, density, and impurities such as air or salt content. It is difficult to measure the true values of the elastic constants due to the almost instantaneous development of creep when ice is loaded. Consequently, the effective elastic constants are found to be dependent on a variety of mechanical parameters such as rate of loading, stress level and grain size (through its influence on the transient creep rate). Gold (1977) has documented experimental results on the influence of grain size, temperature, and rate of loading on the effective Young's modulus. It is found that the effective modulus increases with increase in the rate of loading or grain size.

Two conventional methods exist for the measurement of elastic constants: the static and the seismic methods. Because the time dependent effects are minimized, the seismic method is regarded as being the more accurate, and the elastic constants so measured are termed "dynamic". More recently Gammon et al. (1983) have measured the dynamic elastic moduli of local homogeneous regions in artificial, lake, sea, and glacial ice using the technique of Brillouin spectroscopy. The elastic constants of polycrystalline ice are then determined from the five elastic constants for single crystals.

The dependence of the elastic constants on density and temperature may be explained as follows. A decrease in density or an increase in temperature corresponds to an increase in the oxygen-oxygen distance in the ice lattice and tends to lower the elastic moduli. According to Dantl (1969), a decrease in density by 0.18% corresponds to an increase of the oxygen-oxygen distance by 0.06% and to a decrease in the power constants of the Morse potential by 2%. This explains the decrease in the elastic moduli, which are proportional to the power constant. Gammon et al. (1983) provided an expression for the dependence of the elastic moduli of ice on temperature as follows:

$$X(\theta) = X(\theta_0) (1 - a\theta)/(1 - a\theta_0) \quad (1)$$

where  $X$  denotes an arbitrary elastic modulus at the temperature  $\theta$  (in °C) and  $\theta_0$  denotes the temperature at which  $X$  is known. The constant  $a$  equals  $1.418 \times 10^{-3} (\text{°C})^{-1}$ .

From Gammon et al.'s (1983) measurements, the following elastic parameters for polycrystalline ice at -16 °C were determined: Young's modulus,  $E = 9.332$  GPa; Poisson's ratio,  $\nu = 0.32521$ ; and shear modulus,  $G = 3.521$  GPa. Using these data and Eq. (1), the shear moduli at -10 °C and -40 °C are determined to be 3.492 GPa and 3.638 GPa respectively, an increase of about 4%. Similarly, the Young's moduli at these two temperatures are 9.254 GPa and 9.642 GPa respectively. These findings are in agreement with those of other investigators (see e.g., Gold, 1977). Sinha (1978) and Shyam Sunder and

Wu (1988a,b) have used the value of 9.5 GPa for Young's modulus in their constitutive models.

### 3.2 Steady-State and Transient Creep

Knowledge of the physical mechanisms leading to creep in polycrystalline ice is currently incomplete. Alternative physical mechanisms have been proposed by various researchers in the last decade. Michel (1978) has proposed that creep occurs by dislocation multiplication and the preferred slip of ice crystals on basal planes. Dislocation multiplication in ice has been observed by synchrotron radiation topography (Ahmad et al., 1986). It was argued that the unfavorably oriented crystals will initially rotate to an orientation favoring basal slip, and the overall deformation of the polycrystal is accommodated by local boundary sliding. The model can describe elastic behavior as well as transient and steady-state creep. On the other hand, Sinha (1978) has argued that transient creep (delayed elasticity) is the direct consequence of grain boundary sliding, while steady-state viscous creep is due to basal slip only. Based on the earlier work by Duval et al. (1983), Ashby and Duval (1985) have proposed a kinematic hardening model which satisfies certain dimensional requirements. These requirements were demonstrated to be valid for stresses ranging from 0.1 to 1.47 MPa and for temperatures lying between  $-5^{\circ}\text{C}$  and  $-30^{\circ}\text{C}$  using the data of Jacka (1984). The physical basis of their model is that slip occurs on both basal and nonbasal planes. However, the precise deformation systems have yet to be determined, as discussed in the following.

Duval et al. (1983) have suggested two possibilities for the creep deformation mechanisms. These are based on the results that if extensive creep deformation in a polycrystal is to occur, deformation must occur (i) on at least five independent systems if a uniform state of strain is assumed to exist throughout the polycrystal, or (ii) on at least four independent systems if a self-consistent approach is adopted. Two independent systems are provided by slip on the basal plane, on the systems  $(0\ 0\ 0\ 1) \langle 1\ 1\ 2\ 0 \rangle$ . For the uniform strain assumption, slip must then also occur on the prismatic  $(1\ 0\ 1\ 0) \langle 1\ 1\ 2\ 0 \rangle$  and the pyramidal  $(1\ 1\ 2\ 2) \langle 1\ 1\ 2\ 3 \rangle$  systems. These respectively provide two and one independent systems in addition to the two provided by basal slip. For the self-consistent approach, the two additional systems provided by prismatic shear is sufficient. The other possibility involves basal slip as before, but then basal dislocations climb on prismatic planes to provide two additional systems  $(1\ 0\ 1\ 0) \langle 1\ 1\ 2\ 0 \rangle$ . Again, if uniform strain is assumed, an additional fifth system such as that provided by pyramidal shear must also operate. Since the resistance to slip on nonbasal planes is much larger than that on basal planes (at least sixty times at  $-10^{\circ}\text{C}$ ), as can be inferred from experimental data on the plasticity of monocrystals (Duval et al., 1983), the basal planes initially bear much of the load which is subsequently transferred to the nonbasal planes. This results in transient creep. Steady-state creep results from a balanced interaction between deformations on the basal and nonbasal planes.

### 3.3 Constitutive Modeling of Flow

The discussion above underlines the fundamental differences in the various approaches. More

recently, Shyam Sunder and Wu (1988a, b) have developed a flow model for polycrystalline ice based on thermodynamics with internal state variables as proposed by Coleman and Gurtin (1967). This model departs from previous models in two ways. First, it recognizes that knowledge of the physical mechanisms of creep in polycrystalline ice is incomplete, and consequently describes the plausible mechanisms of creep in terms of certain hard and soft deformation systems. This general approach agrees with that of Sinha (1978), who considers grain boundary sliding (soft) and basal slip (hard) as the operative mechanisms, and Ashby and Duval (1985), who consider basal slip (soft) and nonbasal slip (hard) as the operative mechanisms. Such approach requires phenomenological modeling, thus avoiding details of physical processes which must be confirmed by further theoretical and experimental research. In any case, both Michel's (1978) and Ashby and Duval's (1985) models ultimately resort to a spring-dashpot analogy for modeling of the physical mechanisms. Second, it is consistent with thermodynamic principles. The internal structural change or rearrangement that occurs during creep deformation is accompanied by energy storage and dissipation, and must satisfy the thermodynamic law of dissipation. This important aspect has been largely ignored in previous model development. Furthermore, the model satisfies (i) dimensional requirements at small stresses, i.e., dimensionless creep curves can be constructed from properly non-dimensionalized parameters of time, strain and strain rate (Ashby and Duval, 1985), and (ii) correspondence requirements between constant-stress creep tests and constant strain-rate tests, i.e., a creep curve can be constructed from a family of stress-strain curves, and vice versa (see Mellor and Cole (1983)).

Only small strains and rotations are considered in the model developed by Shyam Sunder and Wu (1988a, b). The total strain rate is additively decomposed into three components associated with elasticity, transient creep and steady state creep. Elastic behavior is described by the classical generalized Hooke's law. The evolution of transient creep is attributed to the generation of certain back and drag stresses that resist the applied stresses. The back stresses are long range elastic stresses which arise from local inhomogeneities such as the polarized distribution of dislocations resulting from dislocation pile-ups at grain boundaries, or stress concentrations at triple points resulting from grain boundary sliding. They represent an anisotropic resistance to flow. On the other hand, the drag stresses are the outcome of short range interactions between dislocations, or the formation of cell walls and kink bands. Dislocation interactions may occur on parallel planes (Taylor hardening) and intersecting planes (Forest hardening). Drag stresses represent an isotropic resistance to flow.

In general, the model considers the internal stresses to be the consequence of the plastic or creep anisotropy of the soft deformation system with respect to the hard deformation system. During loading the reduced stress driving transient creep is the applied stress reduced by the back and drag stresses. Permanent irreversible deformation occurs simultaneously and this is associated with the "steady-state" creep deformation. Upon unloading the back and drag stresses are not instantaneously recovered; rather, they become the driving forces and enable transient creep deformation to be recovered. Thus, an important difference between this model and that of Ashby and Duval (1985) is that transient creep (or anelasticity) is associated directly with the interference of the back and drag stresses on flow processes on



the soft system, while irrecoverable viscous creep is directly associated with steady-state creep.

Power Law Creep.-- The proposed equations are described in the following. For simplicity only the uniaxial equations are considered. Comparison is made with physical models wherever possible. First, additive decomposition of the total strain rate yields:

$$\dot{\epsilon} = \dot{\epsilon}_e + \dot{\epsilon}_t + \dot{\epsilon}_v \quad (2)$$

where  $\epsilon$ ,  $\epsilon_e$ ,  $\epsilon_t$  and  $\epsilon_v$  denote the total strain, the elastic strain, and the transient and steady-state creep strains, respectively. The superposed dot denotes the time derivative. The instantaneous elastic strain is given by the stress divided by Young's modulus. The equation describing steady-state creep at low stresses (e.g., between 0.2 MPa to 2 MPa) is the power law given by:

$$\dot{\epsilon}_v / \dot{\epsilon}_0 = (\sigma/V)^N \quad (3)$$

where  $\dot{\epsilon}_0$  is a reference strain rate (set equal to unity), and  $N$ ,  $\sigma$ , and  $V$  denote the power law index, the stress, and a temperature dependent stress factor, respectively. For the temperature range of approximately  $-40^\circ\text{C}$  to  $-10^\circ\text{C}$ , the stress factor has been found to obey the Arrhenius law:

$$V = V_0 \exp[Q/(NRT)] \quad (4)$$

where  $V_0$ ,  $Q$ ,  $R$  and  $T$  denote a temperature independent constant, the activation energy for steady-state creep, the universal gas constant and the temperature in Kelvin, respectively. The activation energy  $Q$  has been found to lie in the range 60 to 80 KJ mol<sup>-1</sup> within the stated temperature range. Close to the freezing point,  $Q$  increases, possibly due to the effect of grain boundary melting. The power law index  $N$  generally equals three for the stress range described above, although it can vary from one at very low stresses to a value greater than three beyond about 2 MPa. According to the deformation mode map of Goodman et al. (1981), shown in Fig. 3, the deformation mechanism is probably diffusion creep at very low stresses (below  $\sim 0.1$  MPa axial stress at  $-10^\circ\text{C}$  for the grain size of 1 mm), while at higher stresses (above  $\sim 2$  MPa axial stress for the same parameters, and assuming damage or fracture is suppressed) the rate limiting mechanism for dislocation glide is the nucleation of kink pairs. Goodman et al.'s (1981) model is discussed subsequently.

From an analysis of both creep and hardness data Barnes et al. (1971) have used the hyperbolic sine function to describe steady-state creep behavior over the range 0.1 MPa to 10 MPa, corresponding approximately to  $10^{-9} \text{ s}^{-1}$  to  $10^{-2} \text{ s}^{-1}$ , i.e.:

$$\dot{\epsilon}_v / \dot{\epsilon}_o = A' (\sinh \alpha \sigma)^N \exp [-Q/(RT)] \quad (5)$$

where for the temperature range  $-8^\circ\text{C}$  to  $-14^\circ\text{C}$   $\alpha$ ,  $N$ ,  $Q$  and  $A'$  have been determined to be  $0.254 \text{ (MPa)}^{-1}$ ,  $3.08$ ,  $78.1 \text{ KJ mol}^{-1}$  and  $3.14 \times 10^{10} \text{ s}^{-1}$ , respectively.

It is noted that both Eqs. (3) and (5) are phenomenological equations. However, its form is consistent with a physical model of steady-state creep deformation, as proposed by Goodman et al. (1981). This model is motivated by Glen's (1968) idea that the motion of dislocations through the ice lattice is made difficult by the creation of defects (ionic and Bjerrum defects). The hydrogen atoms are believed to be randomly arranged about the oxygen atoms according to the Bernal-Fowler rules. This randomness suggests that for a dislocation to move through the ice lattice, breaches of the rules will be made with the creation of defects. If the randomly arranged protons are frozen on the bonds, Glen (1968) found that the shear stress required to move the dislocation is about a tenth of the shear modulus ( $0.1 \text{ G}$ ), almost equal to the ideal shear strength for ice. As ice creeps at a much lower stress at high homologous temperatures, it is suggested that the protons must be capable of rearrangement to yield a favorable configuration ahead of the dislocation.

Based on Glen's ideas, Frost et al. (1976) and Whitworth et al. (1976) have proposed a kink model in which an initially straight dislocation advances by the nucleation of kink pairs at places where the proton configuration just ahead of the dislocation is favorable. The dislocation is advanced by the drift of the kink pairs which are annihilated when they encounter kinks of opposite sign. Again the advance is possible only when the local proton configuration is favorable.

Goodman et al. (1981) extended their model to include three cases according to temperature or stress level. At low stresses and high homologous temperatures (but above those stress levels at which diffusional creep is dominant) the rate limiting mechanism is proton rearrangement. As the temperature decreases, the rate of proton rearrangement decreases and kink nucleation itself becomes rate limiting. At absolute zero the protons are immobile and the rate limiting mechanism is defect creation itself, with a flow stress close to the ideal strength. The shear strain rate  $\dot{\gamma}$  is given by the Orowan equation:

$$\dot{\gamma} = \rho b v_{\text{dis}} \quad (6)$$

where  $\rho$ ,  $b$  and  $v_{\text{dis}}$  denote the mobile dislocation density, the Burger's vector of dislocation, and the dislocation velocity, respectively.

At low stresses where proton rearrangement is the rate limiting mechanism, Goodman et al. (1981) have used an expression for  $v_{\text{dis}}$  in which  $v_{\text{dis}}$  is inversely proportional to temperature, but proportional to the shear stress  $\sigma_s$  and the term  $\exp[-(F_f + F_m + F_k)/(RT)]$ , where  $F_f$ ,  $F_m$  denote respectively the energies

of formation and motion of a Bjerrum defect, and  $F_k$  is the energy of a kink. Since the energy of kink formation is least on the basal plane, greater on the prismatic plane, and greatest on the pyramidal plane, the dislocation velocities follow a decreasing trend on these planes. With the mobile dislocation density given by

$$\rho = [\sigma_s / (cGb)]^2 \quad (7)$$

where  $c$  is a constant approximately equal to 0.1, the shear strain rate is determined from Eq. (6) as:

$$\dot{\gamma} = a_o (\sigma_s / G)^3 [Gba^2 v_o / (kT)] \exp [-(F_f + F_m + F_k) / (RT)] \quad (8)$$

where  $a$ ,  $v_o$ , and  $k$  denote the kink height, the vibration frequency associated with proton rearrangement, and Boltzmann's constant, respectively. The parameter  $c$  is absorbed in  $a_o$ , which is the only 'empirical' parameter in Eq. (8).

Noting the temperature dependence of  $G$  (see Eq. (1)), and with  $R$  and  $(F_f + F_m + F_k)$  equal to  $8.314 \text{ J mol}^{-1} \text{ K}^{-1}$  and  $78.1 \text{ KJ mol}^{-1}$  respectively, it is readily shown that the variation of the term  $1/(G^2 T)$  with temperature is negligible compared with the corresponding variation in  $\exp [-(F_f + F_m + F_k) / (RT)]$ . For a decrease in temperature from  $-10^\circ\text{C}$  to  $-40^\circ\text{C}$  the inverse term increases by about 7%, while the exponential term decreases by two to three orders of magnitude. Consequently, the power law creep as stated in Eq. (3) is a good approximation of Eq. (8) at low stresses. Indeed, the shear stress and shear strain rate in Eq. (8) can be converted to equivalent axial quantities using the relations  $\dot{\gamma} = (3)^{1/2} \dot{\epsilon}$  and  $\sigma_s = \sigma / (3)^{1/2}$ , and a comparison between Eqs. (3) and (8) then yields:

$$(1/V_o)^3 = a_o b a^2 v_o / (9 G^2 k T) \quad (9)$$

The values of the parameters are provided by Goodman et al. (1981), i.e.:  $a_o = 1.2 \times 10^{-3}$ ,  $a \sim b = 4.52 \times 10^{-10} \text{ m}$ ,  $(1/v_o) = 6.36 \times 10^{-16} \text{ s}$ ,  $k = 1.38 \times 10^{-23} \text{ J K}^{-1}$ . For the temperature at  $T = 263.15 \text{ K}$ ,  $G$  is estimated to be  $3.048 \text{ GPa}$  using an equation contained in Goodman et al. (1981). The parameter  $V_o$  is then estimated to be  $1.20 \text{ KPa}$ , which agrees with the value ( $1.21 \text{ kPa}$ ) used in Shyam Sunder and Wu (1988a, b) for  $Q = 78.1 \text{ KJ mol}^{-1}$ .

At higher stresses (e.g.  $> 2 \text{ MPa}$  at  $-10^\circ\text{C}$ ), kink nucleation becomes rate limiting, and the physical model developed by Goodman et al. (1981) appears to describe well the data presented in Barnes et al. (1971). This model predicts that the shear strain rate tends to infinity as the shear stress approaches the ideal shear strength. However, it should be noted that the physical model is imperfect, since it predicts a

dislocation velocity about an order of magnitude less than that determined experimentally (Frost et al., 1976). More recently, Whitworth (1983) has shown that the predicted and measured values of the dislocation velocity are compatible if basal slip occurs on planes of the glide set (between closely spaced planes of water molecules), instead of on the shuffle set (between widely spaced planes of water molecules) as assumed in the models developed by Frost et al. (1976), Whitworth et al. (1976) and Goodman et al. (1981).

Transient Creep-- Further research is needed for the physical modeling of transient creep in polycrystalline ice. Earlier work by Michel (1978), Sinha (1978), Duval et al. (1983) and Ashby and Duval (1985) has achieved various degrees of link between phenomenology and the physical processes of creep deformation. More recently, Derby and Ashby (1987) have proposed a physical model for 'primary' creep using sub-cell size and misorientation as state variables. It has been applied to the study of primary creep in f.c.c. metals.

In Duval et al. (1983) steady-state creep is considered to be determined by a balance of hardening and recovery processes, and it is suggested that climb of dislocations is a plausible recovery process in polycrystalline ice. The equation for the creep strain rate as proposed by Ashby and Duval (1985) is generally an equation for the transient creep rate. It becomes an equation for the steady-state creep rate when the internal stresses attain their steady state values. In contrast, in the model of Shyam Sunder and Wu (1988a, b) transient creep is associated directly with the generation of back and drag stresses and is generally recoverable. The transient strain rate is described by an independent equation. Recall also that irreversible creep is easily determined since it is associated with steady-state creep and is characterized by the conventional power law.

Both transient and steady-state creep involve the movement of dislocations and their rates can be described by the Orowan equation. Consequently the transient creep can also be phenomenologically characterized by the power law, but with the stress replaced by a reduced stress. The reduced stress in Shyam Sunder and Wu (1988a, b) is taken to be  $(\sigma - R)/B$ , where  $R$  is the back stress and  $B$  is a dimensionless drag stress. The evolution equation for transient creep is then:

$$\dot{\epsilon}_t = [(\sigma - R)/BV]^N \quad (10)$$

where  $V$  is the temperature dependent stress factor given by Eq. (4). Sinha (1978) has determined the activation energy for columnar-grained S-2 ice to be equal to that for steady-state creep. For an evolving structure, evolution equations must also be proposed for  $R$  and  $B$ .

The back stress  $R$  opposes the applied stress and gives rise to directional or kinematic hardening, a much quoted example being the Bauschinger effect in metals. The classical hardening rule of Prager

(1949) relates the rate of back stress linearly to the creep strain rate  $\dot{\epsilon}_{cr}$ . On the other hand, a nonlinear time recovery effect can be introduced by use of the Bailey-Orowan type of relations, i.e.:

$$\dot{R} = h_1 \dot{\epsilon}_{cr} - f_1(R, T) \quad (11)$$

where  $h_1$  is a hardening constant and  $f_1$  is a static recovery function. Equation (11) can be further generalized to include dynamic recovery by requiring  $h_1$  to be a function of the state variables. An equation similar to Eq. (11) has also been used in the physical model of Derby and Ashby (1987), but the recovery function  $f_1$  is expressed as a function of physical parameters pertaining to the assumed physical process of recovery. In the model of Shyam Sunder and Wu (1988a, b) the time rate of the back stress is taken to be linearly related to the transient strain rate, dynamic recovery being implicit in that transient creep is driven by the reduced stress. The uniaxial form of the equation is:

$$\dot{R} = A E \dot{\epsilon}_t \quad (12)$$

where  $A$  is a constant. The parameter  $AE$  may be interpreted as an anelastic modulus. During a creep test, the maximum recoverable strain at steady state (assuming no tertiary creep) is given by  $\sigma/E + \sigma/AE$ , and consequently the applied stress per unit maximum recoverable strain is given by  $EA/(1 + A)$ , which may be interpreted as a relaxed modulus. The initial value of the back stress is taken to be zero for an annealed material or for a material that has recovered from prior loading.

The drag stress, on the other hand, increases the resistance of the material to flow in an isotropic manner. The evolution equation for the drag stress may also take a form similar to Eq. (11), in which the rate of the drag stress is linearly related to the equivalent transient strain rate. In uniaxial form, this equation is:

$$\dot{B} = H E \dot{\epsilon}_t = H E [(\sigma - R)/(BV)]^N \quad (13)$$

where  $H$  is a hardening parameter. However, the mobile dislocation density according to Eq. (7) is proportional to the square of the stress. The rate of drag stress is a measure of the rate of change in isotropic deformation resistance, which increases with increase in the dislocation density. Consequently, the rate of drag stress should also be proportional to the square of the stress. Thus,  $H = \dot{H} / (\sigma - R)$ , i.e., initially the rate of drag stress is proportional to  $\sigma^2$ , while during structural evolution it is proportional to  $(\sigma - R)^2$ . Note that this formulation also leads to a proper dimensionless form of Eq. (13), as shown in Shyam Sunder and Wu (1988a, b). The initial value  $B_0$  represents the isotropic resistance to flow in the initial state of the material.

#### 4. PARAMETER DETERMINATION AND MODEL VALIDATION

The model of Shyam Sunder and Wu (1988a, b) for isotropic polycrystalline ice contains a total of six parameters:  $E$ ,  $N$ ,  $V_0$ ,  $A$ ,  $B_0$  and  $\bar{H}$ . The activation energy  $Q$  is regarded as a property of creep deformation. Except for the Young's modulus, these parameters can be determined from simple constant-stress creep tests or constant strain rate tests. Determination of the first three parameters follows standard procedures. Young's modulus  $E$  can be determined using static or dynamic methods as discussed previously. The power law index  $N$  is generally taken to be three for stresses in the range 0.2 MPa - 2 MPa; this value agrees with theoretical models based on the Orowan equation and the velocity of dislocations. It also agrees with flow stress/strain rate data obtained from constant strain rate tests, as reported in Duval et al. (1983). The activation energy  $Q$  can be determined from minimum creep strain rate data for creep tests conducted at the same load but at different temperatures. Knowing  $Q$  and  $N$ , the stress factor  $V_0$  can then be determined from the flow stress/strain rate data.

The parameter  $AE$  is the anelastic modulus and can be estimated from the maximum transient strain at steady state, i.e.:

$$AE = \sigma / \epsilon_{t, \max} \quad (14)$$

This, however, requires the maximum transient strain to be inferred from the creep data by subtracting the elastic and irrecoverable viscous strain from the total strain (see Fig. 4). An alternative procedure for estimating  $A$  is by measuring the maximum recoverable strain in a creep recovery test, since the applied stress per unit maximum recoverable strain is given by  $EA/(1 + A)$ .

The parameter  $B_0$  has been stated previously as a measure of the initial isotropic deformation resistance to creep (see Fig. 4). Its value can be determined in the following manner. The initial creep strain rate is the sum of the initial transient and irreversible creep strain rates:

$$\dot{\epsilon}_{cr} = (\sigma/V)^N (1 + 1/B_0^N) \quad (15)$$

Measurement of the initial creep rate therefore provides an estimate of  $B_0$ . Finally, the hardening constant  $\bar{H}$  can be estimated from an entire creep curve using the integrated form of Eq. (13) (see Shyam Sunder and Wu (1988a, b)).

To use the numerical model in a predictive mode, it is necessary to verify its predictions. This involves comparing predictions of the constitutive model with experimental data obtained from tests on material specimens, as well as comparing numerical simulations with data obtained from model and field

scale tests. More specifically, the following verification procedures may be followed:

1. To verify the structure of the constitutive model, comparison can be made between model predictions and experimental results for different data sets, which may correspond to either the same or different types of ice. These differences may reflect different grain structures such as columnar-grained ice and granular ice, or the different conditions under which ice specimens are grown. Different ice types may require different sets of material parameters for characterizing their constitutive behavior.
2. Material parameters determined from a specific type of test (e.g. constant-stress test) and for specific test conditions (e.g. at some temperature and stress level) should generate a model prediction reasonably close to the response measured during the test. The robustness of the material parameters should be examined by studying the change in predicted response with change in parameter values. A robust parameter is one in which a small change in the parameter value does not cause significant change in the predicted material response. This is a desirable feature since it creates confidence that gross errors in the model prediction will not occur if a minor inaccuracy happens to occur in the value of a parameter.
3. Material parameters determined from a specific type of test should generate reasonably good predictions of the measured response for the same type of test but for different test conditions. An example is the verification of creep model for different stresses and temperatures (as in Ashby and Duval (1985)). The material behavior and model predictions should be compared for a wide range of the input forcing functions, e.g., applied stress, applied strain rate and temperature. This helps to identify the limitations of the model.
4. The model predictions generated from the same set of parameters should also compare well, or at least consistent in trend, with the measured response for different types of test, e.g., the verification of ice response under variable history loading, cyclic loading (compression-tension, tension-tension, or compression-compression), stress or strain rate jump, and change in confining pressure.
5. The predictions of the numerical model should be verified against model test results. For instance, Sodhi et al. (1983) have verified the results for the buckling loads of wedge-shaped floating ice sheets by comparing experimental data with numerical simulations from a finite element analysis. Consideration should be given to scale effects, especially if the loading conditions permit fracture.
6. Verification with field scale test data should ultimately justify the numerical approach. A validated numerical model can then be used for sensitivity study, or for the predictions of ice response under extreme loading conditions.

## 5. CONCLUSIONS

This paper discusses the building blocks of a numerical model for the study of ice-structure interaction. The relations between the constitutive model, the finite element model, and the system model are examined. Constitutive modeling of polycrystalline ice is discussed in some detail. It is shown that a physically motivated phenomenological model is generally adequate for solving an initial-and boundary-valued problem in a numerical framework. The phenomenological model for steady-state creep, i.e., the power law or the hyperbolic sine function, is compared to a physical model which rests on the assumption that proton rearrangement glide is the rate limiting mechanism in ice. Physical models for transient creep in ice require further development since knowledge of the physical mechanisms of deformation is currently incomplete. Finally, other, but no less important, deformation mechanisms such as

recrystallization and damage, deserve further study. The constitutive modeling of damage processes is currently under investigation by the present authors. It is noteworthy that a physical model for the interactions between two or more deformation mechanisms is currently lacking. Further study of the physical processes of deformation under complex loadings is also needed, e.g., path dependence and cyclic behavior under uniaxial and multiaxial conditions. From the viewpoint of implementation in a numerical framework, it appears that an integration of continuum mechanics with microstructural information currently provides the best approach in constitutive modeling.

#### ACKNOWLEDGEMENTS

The authors would like to acknowledge financial support from BP America, AMOCO, ARCO, CONOCO and MOBIL through MIT's Center for Scientific Excellence in Offshore Engineering, and the U.S. Department of the Interior, Minerals Management Service.

#### REFERENCES

1. Ahmad, S., Ohtomo, M. and Whitworth, R.W. (1986), Observation of a Dislocation Source in Ice by Synchrotron Radiation Topography, *Nature*, Vol. 319, 20, 659 - 660.
2. Ashby, M.F. and Duval, P. (1985), The Creep of Polycrystalline Ice, *Cold Regions Science and Technology*, 11, 285 - 300.
3. Barnes, P., Tabor, D. and Walker, J.C.F. (1971), The Friction and Creep of Polycrystalline Ice, *Proc. Roy. Soc. Lond. A*, 324, 127-155.
4. Boyce, M.C., Parks, D.M. and Argon, A.S. (1988), Large Inelastic Deformation of Glassy Polymers. Part I: Rate Dependent Constitutive Model, *Mechanics of Materials*, 7, 15 - 33.
5. Brown, S.B., Kwon, H.K. and Anand, L. (1988), An Internal Variable Constitutive Model for Hot Working of Metals, *Submitted for Publication*.
6. Coleman, B.D. and Gurtin, M.E. (1967), Thermodynamics with Internal Variables, *Journal of Chemical Physics*, Vol. 47, No. 2, 597 - 613.
7. Dantl, G. (1969), Elastic Moduli of Ice, *Physics of Ice: Proc. Int. Symp. on Phys. of Ice*, Munich, Germany, September 9-14, 1968, in Riehl, N. and others (Eds.), New York, Plenum Press, 223 - 230.
8. Derby, B. and Ashby, M.F. (1987), A Microstructural Model for Primary Creep, *Acta Metallurgica*, Vol. 35, No. 6, 1349 - 1353.
9. Duval, P., Ashby, M.F. and Anderman, I. (1983), Rate-Controlling Processes in the Creep of Polycrystalline Ice, *Journal of Physical Chemistry*, Vol. 87, No. 21, 4066 - 4074.
10. Frost, H.J., Goodman, D.J. and Ashby, M.F. (1976), Kink Velocities on Dislocations in Ice. A Comment on the Whitworth, Paren and Glen Model, *Philosophical Magazine*, Vol. 33, No. 6, 951 - 961.
11. Gammon, P.H., Kieffe, H., Clouter, M.J. and Denner, W.W. (1983), Elastic Constants of Artificial and Natural Ice Samples by Brillouin Spectroscopy, *Journal of Glaciology*, Vol. 29, No. 103, 433 - 460.
12. Glen, J.W. (1968), The Effect of Hydrogen Disorder on Dislocation Movement and Plastic Deformation of Ice, *Phys. Kondens. Mater.*, 7, 43 - 51.
13. Gold, L.W. (1977), Engineering Properties of Fresh-Water Ice, *Journal of Glaciology*, Vol.



- 19, No. 81, 197 - 211.
14. Goodman, D.J., Frost, H.J., and Ashby, M.F. (1981), The Plasticity of Polycrystalline Ice, *Philosophical Magazine A*, Vol. 43, No. 3, 665 - 695.
  15. Jacka, T.H. (1984), The Time and Strain Required for the Development of Minimum Strain Rates in Ice, *Cold Regions Science and Technology*, 8, 261 - 268.
  16. Jordaan, I.J. (1986), Numerical and Finite Element Techniques in Calculation of Ice-Structure Interaction, *Proc. IAHR Symp. on Ice*, Iowa City, Iowa, Vol. II, 405 - 440.
  17. Mellor, M. and Cole, D. (1983), Stress/Strain/Time Relations for Ice Under Uniaxial Compression, *Cold Regions Science and Technology*, 6, 207 - 230.
  18. Michel, B. (1978), A Mechanical Model of Creep of Polycrystalline Ice, *Canadian Geotechnical Journal*, Vol. 15, 155 - 170.
  19. Palmer, A.C., Goodman, D.J., Ashby, M.F., Evans, A.G., Hutchinson, J.W. and Ponter, A.R.S. (1983), Fracture and Its Role in Determining Ice Forces on Offshore Structures, *Annals of Glaciology*, 4, 216 - 221.
  20. Ponter, A.R.S., Palmer, A.C., Goodman, D.J., Ashby, M.F., Evans, A.G., and Hutchinson, J.W. (1983), The Force Exerted by a Moving Ice Sheet on an Offshore Structure, *Cold Regions Science and Technology*, 8, 109 - 118.
  21. Prager, W. (1949), Recent Developments in the Mathematical Theory of Plasticity, *Journal of Applied Physics*, Vol. 20, No. 3, 235 - 241.
  22. Ralston, T.D. (1978), An Analysis of Ice Sheet Indentation, *Proc. I.A.H.R. Symp. on Ice Problems*, Vol I, Lulea, Sweden, 13 - 31.
  23. Rice, J.R. (1971), Inelastic Constitutive Equations for Solids: An Internal- Variable Theory and Its Application to Metal Plasticity, *Journal of the Mechanics and Physics of Solids*, Vol. 19, 433 - 455.
  24. Shyam Sunder, S. and Wu, M.S. (1988a), A Differential Flow Model for Polycrystalline Ice, *Cold Regions Science and Technology*, In Press.
  25. Shyam Sunder, S. and Wu, M.S. (1988b), A Multiaxial Differential Model of Flow in Orthotropic Polycrystalline Ice, *Cold Regions Science and Technology*, In Press.
  26. Shyam Sunder, S., Wu, M.S. and Chen, C.W. (1989), Numerical Modeling of Rate Processes During Ice-Structure Interaction, *Submitted for Publication*.
  27. Sinha, N.K. (1978), Rheology of Columnar-Grained Ice, *Experimental Mechanics*, 18(12), 464 - 470.
  28. Sodhi, D.S., Haynes, D.S., Kato, K. and Hirayama, K. (1983), Experimental Determination of the Buckling Loads on Floating Ice Sheets. *Annals of Glaciology*, Vol. 4, 260 - 265.
  29. Whitworth, R.W. (1983), Velocity of Dislocations in Ice on  $\{0\ 0\ 0\ 1\}$  and  $\{1\ 0\ \bar{1}\ 0\}$  Planes, *Journal of Physical Chemistry*, Vol. 87, No. 21, 4074 - 4078.
  30. Whitworth, R.W., Paren, J.G. and Glen, J.W. (1976), The Velocity of Dislocations in Ice - A Theory Based on Proton Disorder, *Philosophical Magazine*, Vol. 43, No. 3, 409 - 426.

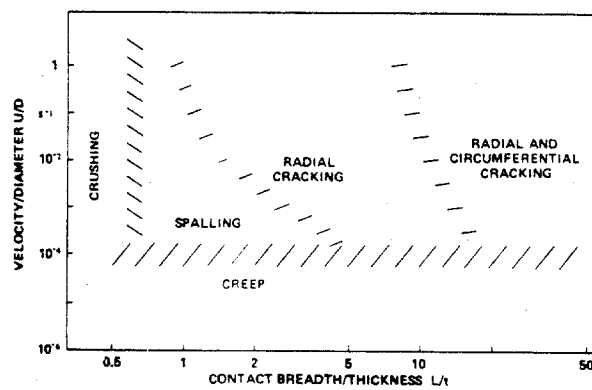
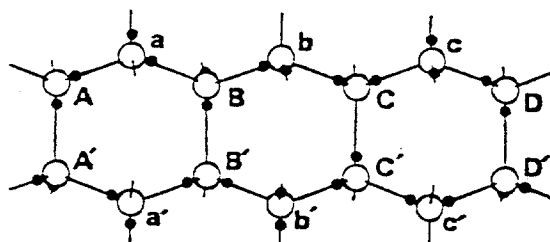
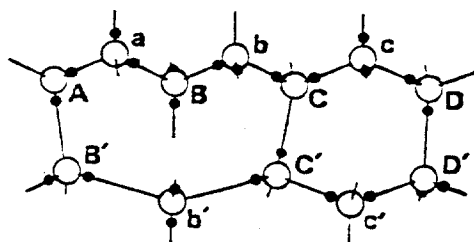


**Fig. 1 Deformation Mode Map**  
(Reproduced From Palmer et al. (1983))

## Ice Lattice Obeying Bernal-Fowler Rules



## Dislocation in Ice Lattice



Bjerrum Defects : D-Defect on B C'; L-Defect on C D'

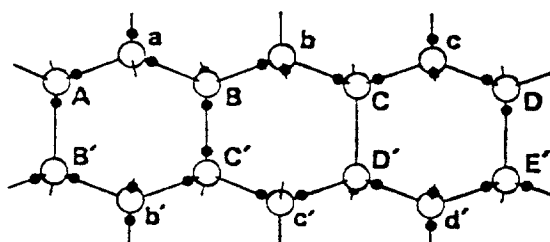


**Fig. 2 Ice Lattice Showing Bjerrum Defects and Dislocation**  
(Reproduced From Glan (1968))

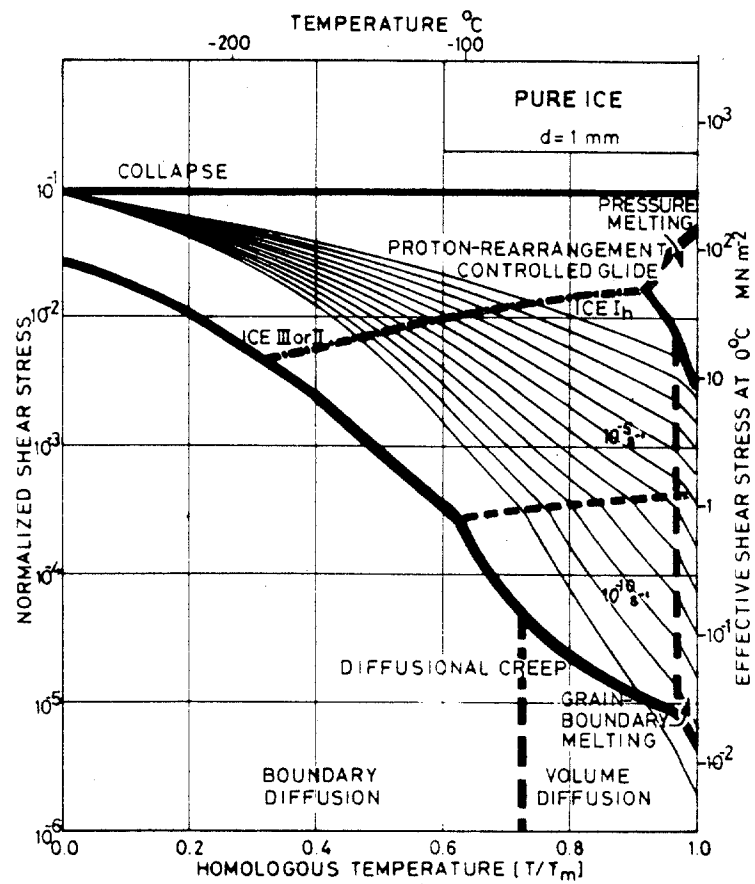


**Fig. 3 Deformation Mechanism Map for Polycrystalline Ice**  
(Reproduced From Goodman et al. (1981))

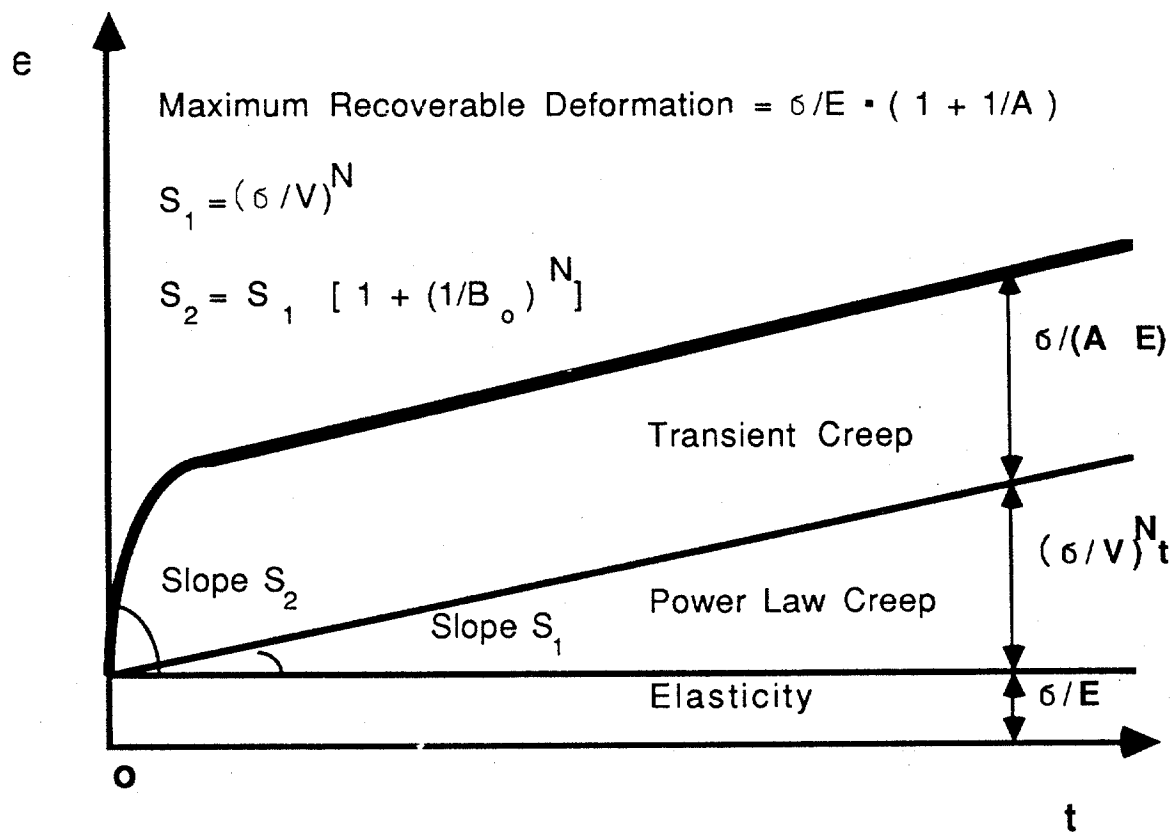


Fig. 4 Identification of Parameters From Constant-Stress Creep Test